In depth characterization of diazotroph activity across the Western Tropical South Pacific hot spot of N$_2$ fixation

Sophie Bonnet[1,2], Mathieu Caffin[1], Hugo Berthelot[1], Olivier Grosso[1,] Mar Benavides[2,3], Sandra Helias-Nunige[2], Cécile Guieu[4,5], Marcus Stenegren[6], Rachel A Foster[6]

[1]IRD, Aix Marseille Université, CNRS/INSU, Université de Toulon, Mediterranean Institute of Oceanography (MIO) UM 110, 13288, Marseille-Nouméa, France-New Caledonia

[2]Mediterranean Institute of Oceanography (MIO) – IRD/CNRS/Aix-Marseille University IRD Nouméa, 101 Promenade R. Laroque, BPA5, 98848, Nouméa cedex, New Caledonia

[3]Marine Biology Section, Department of Biology, University of Copenhagen, 3000 Helsingør, Denmark

[4]Sorbonne Universités, UPMC Université Paris 06, CNRS, Laboratoire d'Océanographie de Villefranche (LOV), 06230 Villefranche-sur-Mer, France

[5]Center for Prototype Climate Modeling, New York University Abu Dhabi, P.O. Box 129188, Abu Dhabi, United Arab Emirates

[6]Department of Ecology, Environment, and Plant Sciences, Stockholm University, Stockholm Sweden 10690

Correspondence to: Sophie Bonnet (sophie.bonnet@univ-amu.fr)

1 **Abstract**

2 Here we report quantification of N_2 fixation rates over a ~4000 km transect in the western and central tropical South

3 Pacific. Water samples were collected along a west to east transect from 160°E to 160°W, covering contrasting trophic

4 regimes, from oligotrophy in the Melanesian archipelagoes (MA) waters to ultra-oligotrophy in the South Pacific Gyre

5 (GY) waters. N_2 fixation was detected at all 17 sampled stations with an average rate of 631 ± 286 µmol N m^{-2} d^{-1}

6 (range 196-1153 µmol N m^{-2} d^{-1}) in MA waters and of 85 ± 79 µmol N m^{-2} d^{-1} (range 18-172 µmol N m^{-2} d^{-1}) in GY

7 waters. Exceptionally high rates of N_2 fixation in MA waters were favored by availability of both iron and phosphate

8 and the observed warm sea surface temperatures (>28°C). *Trichodesmium* and UCYN-B cyanobacteria dominated the

9 diazotroph community (>80 %) and gene expression of nitrogenase genes (cDNA >10^5 *nifH* copies L^{-1}) in MA waters,

10 and single-cell isotopic analyses performed by nanoscale secondary ion mass spectrometry at selected stations reveal

11 that *Trichodesmium* was always the major contributor to N_2 fixation in MA waters, accounting for 47.1 to 83.8 % of

12 bulk N_2 fixation.

13

14

15

16

17

18

19

20

21

22

23

24

25

26

27

28

29

30

31

32

33

34

35

36

37

38

1 Introduction

In the ocean, nitrogen (N) availability in surface waters controls primary production and export of organic matter (Dugdale and Goering, 1967; Eppley and Peterson, 1979; Moore et al., 2013), a process commonly referred to as 'the biological carbon pump'. The major external source of new N to the ocean is biological N_2 fixation (100-150 Tg N yr^{-1}, (Gruber, 2008)), the conversion of N_2 gas dissolved in seawater into ammonia (NH_4^+). This process is performed by diazotrophic organisms possessing the enzyme nitrogenase encoded by the *nifH* genes. This source is continuously counteracted by N losses, mainly driven by denitrification and anammox, which convert fixed N (nitrate, NO_3^-) into N_2. Despite the critical importance of the N inventory in regulating primary production and export, the spatial distribution of N gains and losses in the ocean is still poorly resolved.

A global scale modeling study predicted that the highest rates of N_2 fixation are located in the South Pacific Ocean (Deutsch et al., 2007; Gruber, 2016). These authors also concluded that processes leading to N gains and losses are spatially coupled to oxygen deficient zones such as in the eastern tropical Pacific (ETSP), which harbors NO_3^--poor but phosphate-rich surface waters, i.e. potentially ideal niches for N_2 fixation (Monteiro et al., 2011). However, recent field studies based on several cruises and independent approaches, including biological $^{15}N_2$ incubations-based measurements and geochemical $\delta^{15}N$ budgets, revealed low N_2 fixation rates (average range ~0-60 µmol N m^{-2} d^{-1}) in the surface ETSP waters (Dekaezemacker et al., 2013; Fernandez et al., 2011; Fernandez et al., 2015; Knapp et al., 2016; Loescher et al., 2014), presumably due to iron (Fe) limitation (Bonnet et al., 2017; Dekaezemacker et al., 2013), as Fe is a major component of the nitrogenase enzyme (Raven, 1988). On the opposite, the western tropical South Pacific (WTSP) has recently been identified as a 'hot spot' of N_2 fixation (Bonnet et al., 2017) and together, these studies plead for a basin-wide spatial decoupling between N_2 fixation and denitrification in the South Pacific Ocean.

The WTSP is a vast oceanic region extending from Australia in the west to the western boundary of the South Pacific Gyre in the east (hereafter referred to as GY waters) (Figure 1). It has been chronically undersampled (Luo et al., 2012) compared to the tropical North Atlantic (Benavides and Voss, 2015) and North Pacific (e.g. (Böttjer et al., 2017)) oceans, but recent oceanographic surveys performed in the western part of the WTSP, in the Solomon, Bismarck (Berthelot et al., 2017; Bonnet et al., 2009; Bonnet et al., 2015) and Arafura (Messer et al., 2016; Montoya et al., 2004) Seas report extremely high N_2 fixation rates (>600 µmol N m^{-2} d^{-1}, i.e. an order of magnitude higher than in the ETSP) throughout the year, that have been attributed to sea surface temperature >25°C and continuous nutrient inputs of terrigenous and volcanic origin (Labatut et al., 2014; Radic et al., 2011). The central and eastern parts of the WTSP, a vast oceanic region bordering Melanesian archipelagoes (New Caledonia, Vanuatu, Fiji) up to the Tonga trench (hereafter referred to as MA waters) have been far less investigated. One study (Shiozaki et al., 2014) reported high surface N_2-fixation rates close to Melanesian islands in relation with nutrient supplied by land runoff. However, the lack of direct N_2 fixation measurements over the full photic layer prevents the implementation of N budget estimates in this region. In addition, the reasons for such an ecological success of diazotrophs in the WTSP are still under debate (Bonnet et al., 2017) as the horizontal and vertical distribution of environmental parameters potentially controlling N_2 fixation, in particular Fe concentrations, are still scarce in this region.

Recurrent blooms of the filamentous cyanobacterium *Trichodesmium,* one of the most abundant diazotrophs in our oceans (Luo et al., 2012), have been reported in the WTSP since James Cook and Charles Darwin's expeditions and later confirmed by satellite observations (Dupouy et al., 2011; Dupouy et al., 2000) and microscopic enumerations

1   (Shiozaki et al., 2014; Tenorio et al., Accepted). However, molecular studies based on the *nifH* diversity also revealed

2   the presence of unicellular diazotrophic cyanobacteria (UCYN) in the WTSP (Moisander et al., 2010). Three groups

3   of UCYN (A, B and C) can be distinguished based on *nifH* gene sequences. In the warm (>25°C) waters of the Solomon

4   Sea, UCYN from group B (UCYN-B) co-occur with *Trichodesmium* at the surface, and together dominate the

5   diazotroph community (Bonnet et al., 2015), while UCYN-C are also occasionally abundant (Berthelot et al., 2017).

6   Further south in the Coral and Tasman Seas, UCYN-A dominate the diazotroph community (Bonnet et al., 2015;

7   Moisander et al., 2010). Both studies reported a transition zone from UCYN-B-dominated communities in warm

8   (>25°C) surface waters to UCYN-A-dominated communities in colder (<25°C) waters of the western part of the

9   WTSP. Further east in the MA waters, *Trichodesmium* and UCYN-B co-occur and account for the majority of total

10 *nifH* genes detected (Stenegren et al., 2017). Although molecular methods greatly enhanced our understanding of the

11 biogeographical distribution of diazotrophs in the WTSP, DNA-based *nifH* counts cannot be equaled to metabolic

12 activity. Thus, the contribution of each dominant group to bulk N_2 fixation is still lacking in this globally important

13 'hot spot' of N_2 fixation. Previous studies showed that different diazotrophs have different fates in the ocean: some are

14 directly exported, others release and transfer part of the recently fixed N to the planktonic food web and fuel indirect

15 export of organic matter (Berthelot et al., 2016; Bonnet et al., 2016a; Karl et al., 2012). Consequently assessing the

16 relative contribution of each dominating group of diazotrophs to overall N_2 fixation is critical to assess the

17 biogeochemical impact of N_2 fixation in the WTSP.

18   In the present study, we report previously undocumented bulk and group-specific N_2 fixation quantification

19 over a ~4000 km transect in the western and central tropical South Pacific. The goals of the study were i) to quantify

20 to horizontal and vertical distribution of N_2 fixation rates in the photic layer in relation with hydrological and biological

21 parameters, ii) to quantify the relative contribution of the dominant diazotrophs (*Trichodesmium* and UCYN-B) to N_2

22 fixation at selected stations based on cell-specific measurements, iii) to assess the potential ecological impact of N_2

23 fixation in this region.

24

25 **2   Methods**

26 Samples were collected during the 45-day OUTPACE (Oliotrophic to UlTra oligotrophic PACific Experiment) cruise

27 (DOI: http://dx.doi.org/10.17600/15000900) onboard the R/V *L'Atalante* in February-March 2015 (austral summer).

28 The west to east zonal transect along ~19°S started in Noumea (New Caledonia) and ended in Papeete (French

29 Polynesia) (Figure 1), covering contrasted trophic regimes (oligotrophy to ultra-oligotrophy) (see Moutin et al., 2017

30 for details), crossing MA waters around New Caledonia, Vanuatu, Fiji up to Tonga, and GY waters located at the

31 western boundary of the South Pacific Gyre. Data were collected at 17 stations including 14 short duration (SD; 8 h)

32 stations (SD1 to SD15, note that SD13 was not sampled) and three long duration (LD; 7 days) stations (LDA, LDB

33 and LDC). Vertical (0-200 m) profiles of temperature, salinity, and fluorescence were obtained at all 17 stations using

34 a Seabird 911 plus CTD equipped with a Wetlabs ECO-AFL/FL fluorometer. Seawater samples were collected by 12-

35 L Niskin bottles mounted on the CTD rosette.

36

37

38

2.1 Macro-nutrient and dissolved Fe concentrations analyses

Samples for quantifying nitrate (NO_3^-) and dissolved inorganic phosphorus (DIP) concentrations were collected at 12 depths between 0 and 200 m in acid-washed polyethylene bottles, fixed with $HgCl_2$ (final concentration 20 mg L^{-1}) and preserved at 4°C until analysis. Concentrations were determined using standard colorimetric techniques (Aminot and Kerouel, 2007) on a Bran Luebbe AA3 autoanalyzer. Detection limits for the procedures were 0.05 μmol L^{-1} for NO_3^- and DIP.

The sampling and analytical methods used to analyze the parameters reported in the correlation table (Table 2) are described in details in related papers in this issue (Bock et al., Submitted; Fumenia et al., Submitted; Stenegren et al., 2017; Van Wambeke et al., Submitted). Samples for dissolved Fe (DFe) concentrations determination were collected and analyzed as described in Guieu et al. (Under review).

2.2 Bulk N_2 fixation rate measurements

N_2 fixation rates were measured in triplicate at all 17 stations using the $^{15}N_2$ isotopic tracer technique (adapted from Montoya et al. (1996)). The $^{15}N_2$ bubble technique was intentionally chosen to avoid any potential overestimation due trace metal and dissolved organic matter (DOM) contaminations often associated with the preparation of the $^{15}N_2$-enriched seawater (Klawonn et al., 2015; Wilson et al., 2012) in our incubation bottles as Fe and DOM have been found to control N_2 fixation or *nifH* gene expression in this region (Benavides et al., 2017; Moisander et al., 2011). However, the $^{15}N/^{14}N$ ratio of the N_2 pool available for N_2 fixation (the term A_{N2} used in the Montoya et al. (1996) equation) was measured in all incubation bottles to ensure accurate rate calculations (see below).

Seawater samples were collected in 10 % HCl-washed, sample-rinsed (3 times) light-transparent polycarbonate (2.3 L) bottles from 6 depths (75 %, 50 %, 20 %, 10 %, 1 %, and 0.1% surface irradiance levels) at short-duration stations SD1 to SD15 and 9 depths (75 %, 50 %, 35 %, 20 %, 10 %, 3 %, 1 %, 0.3 % and 0.1 % surface irradiance levels) at LDA, LDB and LDC, corresponding to the sub-surface (5 m) down to 80 to 180 m depending on the station. Bottles were sealed with caps fitted with silicon septa and amended with 2 mL of 98.9 atom% $^{15}N_2$ (Cambridge isotopes). The purity of the $^{15}N_2$ Cambridge isotopes stocks was previously checked by Dabundo et al. (2014) and more recently by (Benavides et al., 2015) and (Bonnet et al., 2016a). They were found to be lower than 2 x 10^{-8} mol:mol of $^{15}N_2$, leading to a potential N_2 fixation rates overestimation of <1 %. Each bottle was agitated for 10 minutes to break the $^{15}N_2$ bubble and facilitate its dissolution and incubated for 24 h. At SD stations, bottles were incubated in on-deck incubators connected to circulating seawater at the specified irradiances using blue screening as the duration of the station (8 h) was too short to deploy in situ mooring lines. At LD stations (7 days), one profile was incubated following the same methodology in on-deck incubators and another replicate profile was incubated in situ for comparison on a drifting mooring line located at the same depth from which the samples were collected. Incubations were stopped by filtering the entire sample onto pre-combusted (450°C, 4 h) 25-mm diameter glass fiber filters (GF/F, Whatman, 0.7 μm nominal pore size), that were dried at 60°C for 24 h before being analyzed for $^{15}N/^{14}N$ ratios and particulate N (PN) concentrations determination using an elemental analyzer coupled to a mass spectrometer (EA-IRMS, Integra CN, SerCon Ltd) as described in (Bonnet et al., 2011).

To ensure accurate rate calculations, the $^{15}N/^{14}N$ ratio of the N_2 pool in the incubation bottles was measured on each profile from triplicate surface incubation bottles from SD1 to SD14 and at all depths at SD15 and LD stations.

1   Briefly, 12 mL were subsampled after incubation into Exetainers® fixed with $HgCl_2$ (final concentration 20 mg L^{-1})

2   that were preserved upside down in the dark at 4°C until analyzed using a membrane inlet mass spectrometer (MIMS)

3   according to (Kana et al., 1994). Lastly, we collected time zero samples at each station to determine the natural N

4   isotopic signature of ambient particulate nitrogen (PN).

5   Discrete N_2 fixation rate measurements were depth integrated over the photic layer using trapezoidal

6   integration procedures assuming that surface N_2 fixation rates were identical to those in subsurface (5 m) and

7   considering that rates below the deepest sampled depth were zero (JGOFS, 1988).

8

9   **2.3**   **Statistical analyses**

10   Spearman's rank correlation was used to examine the potential relationships between N_2 fixation rates, hydrological,

11   biogeochemical, and biological parameters across the longitudinal transect (n=102, α=0.05). A non-parametric Mann-

12   Whitney test (α=0.05) was used to compare the MIMS data obtained following on-deck versus in situ incubations, and

13   to compare nutrient and Chl *a* distributions between the western part and the eastern part of the transect.

14

15   **2.4**   **Group-specific N_2 fixation rate measurements at selected stations**

16   **2.4.1**   **Experimental procedures**

17   At three selected stations along the transect (SD2, SD6, LDB) where *Trichodesmium* and UCYN-B accounted for >90

18   % of the total diazotrophic community (see below and Stenegren et al. (2017)), eight additional polycarbonate (2.3 L)

19   bottles were collected from the surface (50 % light irradiance) to determine *Trichodesmium* and UCYN-B specific N_2

20   fixation rates by nanoSIMS and quantify their contribution to bulk N_2 fixation. Two of them were amended with $^{15}N_2$

21   as described above for further nanoSIMS analyses on individual cells (the 6 remaining bottles were used for DNA and

22   RNA analyses, see below) and were incubated for 24 h with the incubation bottles dedicated to bulk N_2 fixation

23   measurements in on-deck incubators as described above. To recover large-size diazotrophs (*Trichodesmium*) after

24   incubation, 1.5 L were filtered on 10 μm pore size 25 mm diameter polycarbonate filters. The cells were fixed with

25   paraformaldehyde (PFA) (2 % final concentration) for 1 h at ambient temperature (~25 °C) and the filters were then

26   stored at -20°C until nanoSIMS analyses. To recover small size diazotrophs (UCYN-B), samples were collected for

27   further cell sorting by flow cytometry prior to nanoSIMS. 1 L of the remaining $^{15}N_2$ labelled bottle were filtered onto

28   0.2 μm pore size 47 mm polycarbonate filters. Filters were quickly placed in a 5 mL cryotube® filled with 0.2 μm

29   filtered seawater with PFA (2 % final concentration) for 1 h at room temperature in the dark. The cryovials were

30   vortexed for 10 s to detach the cells from the filter (Thompson et al., 2012) and stored at -80°C until cell sorting. Cell

31   sorting of UCYN-B was performed on a Becton Dickinson Influx™ Mariner (BD Biosciences, Franklin Lakes, NJ)

32   high speed cell sorter of the Regional Flow Cytometry Platform for Microbiology (PRECYM), hosted by the

33   Mediterranean Institute of Oceanography, as described in Bonnet et al. (2016a) and (Berthelot et al., 2016). After

34   sorting, the cells were dropped onto a 0.2 μm pore size polycarbonate 13 mm diameter polycarbonate filter connected

35   to low pressure vacuum pump, then stored at -80°C until nanoSIMS analyses. Special care was taken to drop the cells

36   on a surface as small as possible (~5 mm in diameter) to ensure the highest cell density possible to facilitate subsequent

37   nanoSIMS analyses.

38

2.4.2   Abundance of diazotrophs and *nifH* gene expression

The abundance of *Trichodesmium* filaments and the average number of cells/filament was determined microscopically: 1 to 2.2 L were filtered on 2 μm polycarbonate filters. The cells were fixed with PFA (2 % final concentration) for 1 h at 4°C and stored at -20°C until counting using an epifluorescence microscope (Zeiss Axioplan, Jana, Germany) fitted with a green (510–560 nm) excitation filter.

Four other diazotrophic phylotypes were quantified using quantitative PCR (qPCR) as they were too scarce or not enumerable by microscopy: UCYN-A1, UCYN-B and two heterocystous symbionts of diatom-diazotroph associations (DDAs): *Richelia intracellularis* associated with *Rhizosolenia* spp. (het-1) and *Richelia intracellularis* associated with *Hemiaulus* spp. (het-2). Triplicate 2.3 L-bottles were filtered onto 25 mm diameter 0.2 μm Supor filters with a 0.2 μm pore size at each station using a peristaltic pump. The DNA extraction and TaqMAN qPCR assays are fully described in (Stenegren et al., 2017). To evaluate the *nifH* gene expression, additional triplicate 2.3 L bottles were filtered as described above. The filters were placed into pre-sterilized bead-beater tubes (Biospec Products Inc., Bartlesville, OK USA) containing 250 μL RLT buffer (Qiagen RNeasy) amended with 1 % ß-mercaptoethanol and 30 μL of 0.1 mm glass beads (Biospec Products Inc.). The time of filtering for RNA varied between stations (17-21:00). Filters were flash frozen in liquid nitrogen and stored at -80 C until RNA extraction. The RNA extraction and Reverse Transcription were performed as previously described using a Super-Script III first-strand cDNA synthesis kit (Invitrogen Corp., Carlsbad, CA, USA) including the appropriate negative controls (water, and No RT) (Foster et al., 2010).

2.4.3   nanoSIMS analyses, data processing and group-specific rate calculations

NanoSIMS analyses were performed using a nanoSIMS N50 at the French National Ion MicroProbe Facility according to (Bonnet et al., 2016a; Bonnet et al., 2016b) and (Berthelot et al., 2016). Briefly, a ~ 1.3 pA Cesium (16KeV) primary beam focused onto ~100 nm spot diameter was scanned across a 256 x 256 or 512 x 512 pixel raster (depending on the image size) with a counting time of 1 ms per pixel. Samples were pre-sputtered prior to analyses with a current of ~10 pA for at least 2 min to achieve sputtering equilibrium and ensure a consistent implantation and analysis of the cell interior by removing cell surface. Negative secondary ions ($^{12}C^{14}N^-$, $^{12}C^{15}N^-$) were collected by electron multiplier detectors, and secondary electrons were also imaged simultaneously. A total of 10-50 serial quantitative secondary ion images were generated, that were combined to create the final image. Mass resolving power was ~8000 in order to resolve isobaric interferences. 20 to 100 planes were generated for each cells analyzed. NanoSIMS runs are time intensive and not designed for routine analysis, but a minimum of 250 cells of UCYN-B per station and 30 *Trichodesmium* filament portions were analyzed to take into account the variability of activity among the population.

Data were processed using the LIMAGE software. Briefly, all scans were corrected for any drift of the beam and sample stage during acquisition. Isotope ratio images were created by adding the secondary ion counts for each recorded secondary ion for each pixel over all recorded planes and dividing the total counts by the total counts of a selected reference mass. Individual *Trichodesmium* filaments and UCYN-B cells were easily identified on nanoSIMS images that were used to define regions of interest (ROIs). For each ROI, the $^{15}N/^{14}N$ ratio was calculated.

Trichodesmium and UCYN-B cellular biovolume was calculated from cell-diameter measurements performed on 50 ~cells or trichomes per station on an epifluorescence microscope (Zeiss Axioplan, Jana, Germany) fitted with a

Biogeosciences
Discussions

Open Access

EGU

1   green (510–560 nm) excitation filter. UCYN-B had a spherical shape and *Trichodesmium* cells were assumed to have

2   a cylindrical shape. The carbon content per cell was determined from the biovolume according to Verity et al. (1992)

3   and the N content was calculated based on a C:N ratios of 6 for *Trichodesmium* (Carpenter et al., 2004) and 5 for

4   UCYN-B (Dekaezemacker and Bonnet, 2011; Knapp et al., 2012). [15]N assimilation rates were expressed 'par cell' and

5   calculated as follows (Foster et al., 2011; Foster et al., 2013): assimilation (mol N cell^{-1} d^{-1}) = ([15]Nex x N_{con})/N_{sr}, where

6   [15]Nex is the excess ^{15}N enrichment of the individual cells measured by nanoSIMS after 24 h of incubation relative to

7   the time zero value, N_{con} is the N content of each cell determined as described above, and N_{sr} is the excess [15]N

8   enrichment of the source pool (N_2) in the experimental bottles determined by MIMS (see above). Standard deviations

9   were calculated using the variability of N isotopic signature measured by nanoSIMS on replicate cells. The relative

10 contribution of *Trichodesmium* and UCYN-B to bulk N_2 fixation was calculated by multiplying cell-specific N

11 assimilation by the cell abundance of each group, relative to bulk N_2 fixation determined at the same time.

12

13 **3   Results**

14 **3.1   Environmental conditions**

15 Seawater temperature ranged from 21.4 to 30.0 °C in the sampled photic layer (0 to ~80-180 m) over the cruise transect

16 (Figure 2a). Maximum temperatures were measured at the surface (0-50 m, 28.7 °C on average) and remained constant

17 along the longitudinal transect, with one exception when slightly higher sea surface temperatures (SST) were observed

18 at LDB (29.9°C) compared to the transect average SST (28.7°C).

19   For nutrients, DFe and Chl *a* concentrations, the transect was divided into two main characteristic sub-regions:

20 1) the MA region from station SD1 (160°E) to LDB (165°W), and 2) the GY sub-region from station LDB (165°W)

21 to SD15 (160°W) located in the South Pacific Gyre. Chl *a* concentrations were significantly (p<0.05) higher in MA

22 waters (0.17 µg L^{-1} on average over 0-50 m) than in GY waters (0.06 µg L^{-1} on average over 0-50 m) (Figure 1, Figure

23 2b). The DCM was located around 80-100 m in MA waters and deepened at ~150 m in GY waters. Surface NO$_3^-$

24 concentrations (Figure 2c) were close or below the detection limit (0.05 µmol L^{-1}) all over the surface (0-50 m) waters

25 throughout the transect, but the depth of the nitracline gradually deepened from ~80-100 m in MA waters down to

26 ~150 m in GY waters. DIP concentrations were slightly higher or close to detection limits (0.05 µmol L^{-1}) in MA

27 surface (0-50 m) waters and increased significantly (p<0.05) in GY waters to reach 0.13-0.17 µmol L^{-1} (Figure 2d).

28

29 **3.2   N isotopic signature of the N_2 pool after incubation (MIMS results)**

30 The ^{15}N enrichment of the N_2 pool after 24 h of incubation with the [15]N_2 tracer was on average 6.145 ± 0.798 atom%

31 (n=54) in bottles incubated in on-deck incubators and significantly higher (p<0.05) in bottles incubated on the in situ

32 mooring line (7.548 ± 0.557 atom% (n=44), Figure 3a). However, the depth of incubation on the in situ mooring line

33 (between 5 and 180 m) did not have any significant effect (p>0.05) on the isotopic signature of the N_2 pool at LDB

34 and LDC, which remained constant over the water column (Figure 3b).

35

36 **3.3   Natural isotopic signature of suspended particles and N_2 fixation rates**

37 The ^{15}N/^{14}N ratio of suspended particles measured over the photic layer was on average -0.41‰ in MA waters and

38 8.06‰ in GY waters (Table 1). Those numbers were used as time zero samples to calculate N_2 fixation rates.

1   N$_2$ fixation was detected at all 17 sampled stations and the transect could also be divided into the two main

2   characteristic sub-areas: 1) the MA waters exhibiting average N$_2$ fixation rates of 8.9 ± 10 nmol N L^{-1} d^{-1} (range: DL-

3   48 nmol N L^{-1} d^{-1}) over the photic layer, and 2) the GY waters exhibiting average N$_2$ fixation rates of 0.5 ± 0.6 nmol

4   N L^{-1} d^{-1} (range: 0-4.0 nmol N L^{-1} d^{-1}) (Figure 2e). In MA waters, N$_2$ fixation was mostly restricted to the surface (0-

5   25 m), where rates commonly peaked at 30 to 48 nmol N L^{-1} d^{-1}. In GY waters, maximum rates reached 1-2 nmol N

6   L^{-1} d^{-1} and were located deeper in the water column (~50 m). When integrated over the photic layer, N$_2$ fixation

7   represented an average net N addition of 631 ± 286 µmol N m^{-2} d^{-1} (range 196-1153 µmol N m^{-2} d^{-1}) in MA waters

8   and of 85 ± 79 µmol N m^{-2} d^{-1} (range 18-172 µmol N m^{-2} d^{-1}) in GY waters.

9

10   **3.4   Correlations between N$_2$ fixation and hydrological, biogeochemical and biological parameters**

11   N$_2$ fixation rates were significantly positively correlated with seawater temperature and photosynthetically active

12   radiation (PAR) ($p < 0.05$) and significantly negatively correlated with depth and salinity ($p < 0.05$) and not significantly

13   correlated with dissolved oxygen concentrations ($p > 0.05$) (Table 2). Regarding the main biogeochemical stocks and

14   fluxes measured during the cruise, N$_2$ fixation rates were significantly positively correlated with dissolved organic N

15   (DON), phosphorus (DOP) and carbon (DOC), particulate organic N (PON), particulate organic carbon (POC),

16   biogenic silica (BSi) and Chl a concentrations ($p < 0.05$) and significantly negatively correlated with NO$_3^-$, NH$_4^+$, DIP

17   and silicate concentrations ($p < 0.05$).

18   In terms of diazotrophic groups based on the quantification of *nifH* genes by qPCR (Stenegren et al., 2017),

19   N$_2$ fixation rates were significantly positively correlated with *Trichodesmium* spp., UCYN-B and the three DDAs (het-

20   1, het-2 and het-3) abundances ($p < 0.05$) and not significantly correlated with UCYN-A1 and UCYN-A2 abundances

21   ($p > 0.05$) (Table 2). Regarding non-diazotrophic plankton determined by flow cytometry (Bock et al., Submitted), N$_2$

22   fixation rates were significantly positively correlated with *Prochlorococcus* spp., *Synechococcus* spp., heterotrophic

23   bacteria and protists abundances ($p < 0.05$) and significantly negatively correlated with picoeukaryotes ($p < 0.05$).

24

25   **3.5   Contribution of *Trichodesmium* and UCYN-B to N$_2$ fixation and nitrogenase gene expression**

26   At the three stations where cell specific N$_2$ fixation rates were estimated by nanoSIMS (SD2, SD6 and LDB), the most

27   abundant diazotroph phylotype was *Trichodesmium* with 1.3×10^5, 3.3×10^5 and 1.2×10^5 cells L^{-1} respectively,

28   followed by UCYN-B, which abundances were 2.0×10^4, 1.5×10^5 and 3.8×10^2 *nifH* copies L^{-1} respectively. Het-1

29   and het-2 combined were one to two orders of magnitude lower, ranging from 1.0 to 9.9×10^3 *nifH* copies L^{-1} and

30   UCYN-A1 were below detection at the three stations. In summary, *Trichodesmium* and UCYN-B accounted for 98.2

31   %, 99.8 % and 92.1 % of the total diazotroph community (based on the phylotypes targeted here) at SD2, SD6 and

32   LDB, respectively (Table 3).

33   The ^{15}N/^{14}N ratio of individual cells/trichomes of UCYN-B and *Trichodesmium* were measured via nanoSIMS

34   analyses and used to estimate single cell N$_2$ fixation rates. A summary of the enrichment values and cell-specific N$_2$

35   fixation is provided in Table 3. Individual trichomes exhibited significant ^{15}N enrichments (0.610 ± 0.269, $0.637 \pm$

36   0.355 and 0.981 ± 0.466 atom% at stations SD2, SD6 and LDB, respectively) compared with time zero samples (0.369

37   ± 0.002 atom%). UCYN-B were also significantly ^{15}N-enriched with 1.163 ± 0.531 atom% and 0.517 ± 0.237 atom%

38   at SD2 and SD6, respectively (no UCYN-B could be sorted and analyzed by nanoSIMS at LDB as they accounted for

1   only 0.3 % of the diazotroph community). Cell-specific N_2 fixation of *Trichodesmium* were 38.9 ± 8.1, 29.3 ± 5.4 and

2   123.8 ± 24.8 fmol N cell d^{-1} at SD 2, SD6 and LDB. Cell-specific N_2 fixation of UCYN-B were 30.0 ± 6.4 and 6.1 ±

3   1.2 fmol N cell d^{-1} at SD1 and SD6. The contribution of *Trichodesmium* to bulk N_2 fixation was 83.8 %, 47.1 % and

4   52.9 % at stations SD2, SD6 and LDB, respectively. The contribution of UCYN-B was 10.1 %, 6.1 % at SD2 and SD6,

5   respectively (Table 3).

6   The *in situ nifH* expression for all diazotroph groups targeted by qPCR was estimated using a TaqMAN

7   quantitative reverse transcription PCR (RT-QPCR) (Table 4). The sampling and filtering time (17-21:00 h) was not

8   optimal for quantifying the *nifH* gene expression for all diazotrophs, however it is useful evaluation for which

9   diazotrophs were active during the experiment. Both *Trichodesmium* and UCYN-B dominated the biomass (Stenegren

10 et al., 2017), as did their *nifH* gene expression at all three stations, especially SD2 and SD6. Of the two het-groups,

11 het-1 had a higher *nifH* gene expression, which was consistent with its higher *nifH* abundance by standard qPCR

12 (Stenegren et al., 2017). UCYN-A1 was consistently below detection for the *nifH* gene expression and was also the

13 least detected diazotroph by *nifH* qPCR.

14

15 **4   Discussion**

16 **4.1   Methodological considerations: the importance of measuring the $^{15}N/^{14}N$ ratio of the N_2 pool**

17 Our understanding of the marine N cycle relies on accurate measurements of N fluxes to and from the ocean. Two

18 methods are routinely used by the scientific community to perform direct N_2 fixation measurements in marine systems:

19 1) the method developed by (Montoya et al., 1996), which consists of the addition of the $^{15}N_2$ tracer as a bubble in the

20 incubation bottles (hereafter referred to as the 'bubble addition method') and the measurement of the $^{15}N/^{14}N$ ratio of

21 PN before (time zero) and after incubation, 2) the method consisting of adding the $^{15}N_2$ as dissolved in a subset of

22 seawater previously N_2 degassed (Mohr et al., 2010) (hereafter referred to as the '$^{15}N_2$-enriched seawater method').

23 The second method was developed because the first had been observed to potentially underestimate N_2 fixation rates

24 (Großkopf et al., 2012; Mohr et al., 2010; Wilson et al., 2012) due to the incomplete (and gradually increasing during

25 the incubation period) equilibration of the $^{15}N_2$ in the incubation bottles when injected as a bubble. This results in a

26 lower $^{15}N/^{14}N$ ratio of the N_2 pool available for N_2 fixation (the term A_{N2} used in the Montoya et al. (1996) equation)

27 as compared to the theoretical value calculated based on gas constants, and therefore potentially leads to

28 underestimated rates in some studies (see references above), whereas other studies do not see any significant

29 differences between both methods (Bonnet et al., 2016c; Shiozaki et al., 2015). Here we decided to use the 'bubble

30 addition method' to minimize potential trace metal and organic matter contaminations, which may have resulted in

31 overestimating rates (Klawonn et al., 2015). However, we paid careful attention to accurately measure the term A_{N2} to

32 avoid any potential underestimation and reveal that the way bottles are incubated (on-deck *versus* in situ) has a great

33 influence of the A_{N2} value, and thus on N_2 fixation rates.

34   Our MIMS results reveal a significantly (p<0.05) lower ^{15}N enrichment of the N_2 pool (6.145 ± 0.798 atom%)

35 when bottles were incubated in on-deck incubators compared to when bottles were incubated on the in situ mooring

36 line (7.548 ± 0.557 atom%). This suggests that the $^{15}N_2$ dissolution is much more efficient when bottles are incubated

37 in situ, probably due to the higher pressure in seawater at the depth of incubation (1.5 to 19 bars between 5 and 180

38 m) compared to the pressure in the on-deck incubators (1 bar). The seawater temperature checked regularly in the on-

1   deck incubators was equivalent to ambient SST and likely did not explain the differences observed. This result

2   highlights the need to perform systematic MIMS measurements to use the most accurate A_{N2} value for rate calculations,

3   independently of the $^{15}N_2$ approach used (gas or dissolved). In our study, the theoretical A_{N2} value based on gas

4   constants calculations (Weiss, 1970) was ~8.2 atom%, so the deviation from this value is more important when bottles

5   are incubated in on-deck incubators as compared to when they are incubated in situ. This suggests that the use of the

6   bubble addition method without MIMS measurement potentially leads to higher underestimations when bottles are

7   incubated in on-deck incubators, which is the case in the great majority of marine N_2 fixation studies published so far

8   (Luo et al., 2012). We are aware the dissolution kinetics of $^{15}N_2$ in the incubation bottles may have been progressive

9   along the 24 h of incubation (Mohr et al., 2010), therefore, the N_2 fixation rates provided here represent conservative

10 values.

11   Despite the A_{N2} value differed according to the incubation mode, it did not change with the depth of incubation

12 on the mooring line, indicating that a slightly higher pressure than atmospheric pressure (1.5 bar at 5 m depth) is

13 enough to promote the $^{15}N_2$ dissolution. In our study, the vertical profiles performed at LD stations and incubated either

14 on-deck in triplicate or in situ in triplicates reveal identical ($p>0.05$) N_2 fixation rates regardless of the incubation

15 method used (Caffin et al., 2017). This indicates that in situ incubations and under in situ-simulated conditions (on-

16 deck incubators) is a valid methodology for $^{15}N_2$ rate measurements on cruises during which in situ mooring lines

17 cannot be deployed, as long as systematic measurements of the isotopic ratio of the N_2 pool is performed in incubation

18 bottles.

19

20 **4.2   What causes such a hot spot of N_2 fixation in the WTSP?**

21 N_2 fixation rates measured in MA waters (average 631 ± 286 μmol N m^{-2} d^{-1}) are three to four times higher than model

22 predictions for this area (150-200 μmol N m^{-2} d^{-1}, Gruber (2016)). They are in the upper range of the upper category

23 (100-1000 μmol N m^{-2} d^{-1}) of rates defined by (Luo et al., 2012) in the global N_2 fixation MAREDAT database and

24 thus reveal the WTSP as a 'hot spot' of N_2 fixation in the global ocean. Recent studies performed in the western part

25 of the WTSP, ie. in the Solomon, Bismarck (Berthelot et al., 2017; Bonnet et al., 2009; Bonnet et al., 2015) and Arafura

26 (Messer et al., 2015; Montoya et al., 2004) Seas also reveal extremely high rates (>600 μmol N m^{-2} d^{-1}), indicating that

27 this 'hot spot' of N_2 fixation extends geographically west-east from Australia to Tonga and north-south from the

28 equator to 25-30°S, covering a vast ocean area of ~13 x 10^6 km^2 , (i.e. ~20 % of the South Pacific Ocean area).

29 However, the reasons for such an ecological success of diazotrophs in this region are still poorly understood and raise

30 the question of 'which factors influence the distribution and activity of N_2 fixation in the ocean?' In a study conducted

31 in 2014 at global scale, Luo et al. (2014) investigated the statistical links between the spatial variation of N_2 fixation

32 and that of environmental parameters commonly accepted to control this process: surface NO_3^- and DIP concentrations,

33 the tracer P*, atmospheric deposition, sea surface temperature (SST), mixed layer depth, solar radiation in the mixing

34 layer, wind speed and minimum oxygen concentration in the 0-500 m layer. They concluded that the best predictor to

35 explain the spatial distribution of N_2 fixation in the ocean is SST (or surface solar radiation). Below we highlight the

36 most plausible factors explaining this 'hot spot' of N_2 fixation.

37   **SST**. SST was unlikely the factor explaining the differences in N_2 fixation rates observed between MA and

38 GY waters, as SST was consistently high (28.7°C on average over the 0-50 m layer) and optimal for the growth and

1 nitrogenase activity of most diazotrophs (Breitbarth et al., 2007; Fu et al., 2014) all along the cruise transect. This

2 indicates that other factors such as nutrient availability may explain the distribution of N_2 fixation.

3 **DIP availability**. The ~4000 km transect was clearly divided into two main sub-regions: 1) the MA waters,

4 harboring typical oligotrophic conditions with surface (0-50 m) NO_3^- and DIP concentrations close to detection limits

5 (0.05 µmol L^{-1}), moderate surface (0-50 m) Chl a concentrations (~0.17 µg L^{-1}), a DCM located at ~80-100 m and

6 very high N_2 fixation rates (631 ± 286 µmol N m^{-2} d^{-1} on average), 2) the GY waters harboring ultra-oligotrophic

7 conditions with undetectable NO_3^-, high DIP concentrations (0.15 µmol L^{-1}), very low Chl a concentrations (0.06 µg

8 L^{-1}, DCM ~150 m) and low N_2 fixation rates (85 ± 79 µmol N m^{-2} d^{-1}).

9 In the NO_3^--depleted MA waters, the DIP concentrations close to the detection limit are indicative of the

10 consumption of DIP by diazotrophs. This is consistent with the negative correlation found between N_2 fixation and

11 DIP turn-over time (T_{DIP}, the ratio between DIP concentrations and DIP uptake rates) during the OUTPACE cruise

12 (Table 2), indicative of higher DIP limitation when N_2 fixation increases and consume DIP. On the opposite, DIP

13 concentrations are high (>0.1 µmol L^{-1}) in GY surface waters, consistent with former studies considering the South

14 Pacific Gyre as a High Phosphate, Low Chlorophyll ecosystem (Moutin et al., 2008), in which DIP accumulates in the

15 absence of NO_3^- and low N_2 fixation activity, which is suspected to be limited by temperature and/or Fe availability

16 (Bonnet et al., 2008; Moutin et al., 2008). Moutin et al., (2005) have shown that seasonal variations in DIP availability

17 control the growth and decline of *Trichodesmium* blooms in New Caledonian waters. During the OUTPACE cruise,

18 T_{DIP}s were variable in MA waters but always much higher than those typically measured in severely DIP-limited

19 environments such as the Mediterranean and the Sargasso Seas (e.g. (Moutin et al., 2008)), suggesting that DIP

20 concentrations are generally favorable for the development of diazotrophs in the WTSP, and do not alone explain why

21 N_2 fixation is high in MA waters and low in GY waters. However, it is likely that the depletion of DIP stocks at the

22 end of the summer season forces the decline of diazotrophic blooms in the WTSP (Moutin et al., 2005), concomitantly

23 with the decline in SST.

24 **Fe availability**. Before OUTPACE, our knowledge on Fe sources and concentrations in the WTSP was

25 patchy, especially in MA waters. During OUTPACE, Guieu et al. (Under review) reported high DFe concentrations in

26 MA waters (1.7 nmol L^{-1} on average over the photic layer), i.e significantly (p<0.05) higher than those reported in GY

27 waters (0.3 nM on average over the photic layer). The low DFe concentrations measured in the GY waters are in

28 accordance with previous reports for the same region (Blain et al., 2008; Fitzsimmons et al., 2014). However, the high

29 DFe concentrations measured in MA waters were previously undocumented, and reveal several maxima (> 50 nmol

30 L^{-1}) between stations SD7 to SD11, suggesting intense fertilization processes taking place in this region. Guieu et al.

31 (Under review) found that atmospheric deposition in this region was too low to explain the observed DFe

32 concentrations in the water column, and that the Fe inputs up to the euphotic layer is from a shallow (~500 m)

33 hydrothermal source. The seafloor of the WTSP hosts the Tonga-Kermadec subduction zone which stretches 2500 km

34 from New Zealand to the Tonga archipelago. It has among the highest density of submarine volcanoes associated with

35 hydrothermal vents recorded in the ocean (2.6 vents/100 km; Massoth et al. (2007)), which discharge large quantities

36 of material into the water column, including biogeochemically relevant elements such as Fe, manganese, etc. By use

37 of modeling simulations, Guieu et al., (Under review) hypothesize that such shallow Fe sources could spread

38 throughout the WTSP through mesoscale activity and mainly predominant westward currents such as the South

1 Equatorial Current, SEC (Figure 1) and thus explain the high DFe concentrations in MA waters compared to the GY

2 ones. In our study, DFe concentrations were significantly positively correlated with N_2 fixation, likely contributing to

3 explaining the contrasted N_2 fixation rates observed across the OUTPACE transect. This is in accordance with recent

4 model simulations performed at the Pacific scale, which show that deep Fe sources controls the spatial distribution and

5 the abundance of *Trichodesmium* in the WTSP (Dutheil et al., Submitted).

6 Our hypothesis to explain the spatial distribution of N_2 fixation in this region is the following: when DIP-rich

7 waters flow westward from the ETSP through the SEC and cross the South Pacific Gyre, N_2-fixing organisms do not

8 develop despite optimal SST (>25°C), likely because GY waters are Fe-depleted (Bonnet et al., 2008; Moutin et al.,

9 2008). When these DIP-rich waters pass the Tonga trench, the high DFe concentrations associated with SST >25°C

10 altogether would provide ideal conditions for diazotrophs to bloom extensively and likely explain the 'hot spot' of N_2

11 fixation in the region. Further investigations are required to better quantify Fe input from shallow volcanoes and

12 associated hydrothermal activity along the Tonga volcanic arc for the upper mixed layer, study the fate of hydrothermal

13 plumes in the water column at the local and regional scales, and investigate the potential impact of such hydrothermal

14 inputs on diazotrophic communities at the scale of the whole WTSP.

15 Besides DFe, N_2 fixation rates were significantly negatively correlated with depth, which likely explains the

16 significantly positive correlations between N_2 fixation and PAR and N_2 fixation and seawater temperature, those two

17 parameters being also depth dependent (the thermocline was roughly located around 50 m). N_2 fixation rates were the

18 highest were NO_3^- concentrations were the lowest, and both were significantly negatively correlated, consistent with

19 the high energetic cost of N_2 fixation compared to NO_3^- assimilation (Falkowski, 1983).

20

21 **4.3   *Trichodesmium*: the major contributor to N_2 fixation in the WTSP**

22 In this 'hot spot' of N_2 fixation (MA waters), the dominant diazotroph phylotypes quantified using *nifH* quantitative

23 PCR assays were *Trichodesmium* spp. and UCYN-B (Stenegren et al., 2017), which commonly peaked at >10^6 *nifH*

24 copies L^{-1} in surface (0-50 m) waters. DDAs (mainly het-1, but het-2 and het-3 were also detected) were the next most

25 abundant diazotrophs (Stenegren et al., 2017). This result is consistent with the fact that abundances of those four

26 phylotypes co-varied and were significantly positively correlated with N_2 fixation rates (Table 2). The two UCYN-A

27 lineages (UCYN-A1 and UCYN-A2) were less abundant (<1.0-1.5 % of total *nifH* copies, Stenegren et al., 2017) and

28 not significantly correlated with N_2 fixation rates (Table 2).

29 The relative contribution of different diazotroph phylotypes to bulk N_2 fixation has been largely investigated

30 through bulk and size fractionation measurements (usually comparing > and <10 µm size fraction N_2 fixation rates),

31 which may be misleading since some small-size diazotrophs are attached to large-size particles (Benavides et al., 2016;

32 Bonnet et al., 2009) and some diazotrophic-derived N released by diazotrophs is assimilated by small and large non-

33 diazotrophic plankton (e.g. Bonnet et al. (2016a)). Here we directly measure the *in situ* cell-specific N_2 fixation activity

34 of the two diazotroph groups dominating the community in MA waters: *Trichodesmium* and UCYN-B.

35 At all three studied stations, *Trichodesmium* was dominating, accounting for 68.0-91.8 % of the diazotroph

36 community, followed by UCYN-B, accounting for 0.3 to 31.7 %. Likewise *Trichodesmium* and UCYN-B had the

37 highest gene expression (10^2-10^5 cDNA *nifH* copies L^{-1}). It was not surprising that UCYN-B had high gene expression

38 given that the sampling time occurred later in the day (17-21:00), however both *Trichodesmium* and het-1 which

Biogeosciences
Discussions

EGU
Open Access

1   typically reduce N$_2$ and express *nifH* highest during the day (Church et al. 2005), had detectable and often equally high

2   expression as UCYN-B. Cell-specific N$_2$ fixation rates reported here are in the same order of magnitude as those

3   reported for field populations of *Trichodesmium* (Berthelot et al., 2016; Martinez-Perez et al., 2016) and UCYN-B

4   (Foster et al., 2013). *Trichodesmium* was always the major contributor to N$_2$ fixation, accounting for 47.1 to 83.8 % of

5   bulk N$_2$ fixation, while UCYN-B never exceeded 6.1-10.1 %, despite accounting for >30 % of the diazotroph

6   community at SD6. This may be linked with the lower ^{15}N enrichment at SD6 (0.517 ± 0.237 atom%), which is due to

7   a high proportion of inactive cells (atom% close to natural abundance) compared to SD2, where the majority of cells

8   were active and highly ^{15}N-enriched (1.163 ± 0.531 atom%). Such heterogeneity in N$_2$ fixation rates among cells has

9   already been reported by Foster et al., (2013). Overall, these results show that the most abundant phylotype

10   (*Trichodesmium*) accounts for the majority of N$_2$ fixation, but not in the same proportion, highlighting that the

11   abundance of micro-organisms in seawater cannot be equated to activity, which has already been reported for other

12   functional groups such as bacteria (Boutrif et al., 2011). In the North Pacific Gyre (Station ALOHA), Foster et al.

13   (2013) report a higher contribution of UCYN-B to bulk N$_2$ fixation (24-63 %) during the summer season, indicating

14   that this group likely contributes more to the N budget at station ALOHA than in the WTSP, where *Trichodesmium*

15   seems to be the major player.

16

17   **4.4   Ecological relevance of N$_2$ fixation in the WTSP**

18   N$_2$ fixation was significantly positively correlated with Chl *a*, PON, POC and BSi concentrations, as well as with

19   primary production, suggesting a tight coupling between N$_2$ fixation, primary production and biomass accumulation

20   in the water column. Based on our measured C:N ratios at each depth, the computation of the N demand derived from

21   primary production measured during OUTPACE (Van Wambeke et al., Submitted) indicates that N$_2$ fixation fueled on

22   average 8.2 ± 1.9 % (range 5.9 to 11.5 %) of total primary production in the WTSP. This contribution is higher than

23   in other oligotrophic regions such as the Northwestern Pacific (Shiozaki et al., 2013), ETSP (Raimbault and Garcia,

24   2008), Northeast Atlantic (Benavides et al., 2013b) or the Mediterranean Sea (Bonnet et al., 2011; Ridame et al., 2013),

25   where it is generally <5 %. However, it is comparable to results found further North in the Solomon Sea (N$_2$ fixation

26   fueled 9.4 % of primary production, Berthelot et al. (2017)), which is part of the WTSP 'hot spot' of N$_2$ fixation

27   (Bonnet et al., 2017). Caffin et al. (2017) show that N$_2$ fixation represents the major source (>90 %) of new N to the

28   upper photic (productive) layer during the OUTPACE cruise, before atmospheric inputs and nitrate diffusion across

29   the thermocline, indicating that N$_2$ fixation supported nearly all new production in this region during austral summer

30   conditions.

31   The large amount of N provided by N$_2$ fixation likely stimulated the growth of non-diazotrophic plankton

32   as suggested by significant positive correlations between N$_2$ fixation rates and the abundance of *Prochlorococcus* spp.,

33   *Synechococcus* spp., heterotrophic bacteria and protists. ^{15}N$_2$ based transfer experiments coupled with nanoSIMS

34   experiments designed to trace the passage of ^{15}N in the planktonic food web demonstrated that ~10 % of diazotroph-

35   derived N is rapidly (24-48 h) transferred to non-diazotrophic phytoplankton (mainly diatoms and bacteria) in coastal

36   waters of the WTSP (Bonnet et al., 2016a,b; Berthelot et al., 2016). The same experiments performed in offshore

37   waters during the present cruise confirm that ~10 % of recently-fixed N$_2$ are also transferred to picophytoplankton and

38   bacteria after 48 h (Caffin et al., Submitted). This is in accordance with Van Wambeke et al., Submitted) who report

1   that N_2 fixation fuels 30 to 70 % of the bacteria N demand in MA waters. This further demonstrates that N_2 fixation

2   acts as an efficient natural N fertilization in the WTSP, potentially fueling subsequent export of organic material below

3   the photic layer. Caffin et al. (2017) estimated that the e-ratio, which quantifies the efficiency of a system to export

4   particulate carbon relative to primary production (e-ratio = POC export/PP), was three times higher ($p<0.05$) in MA

5   waters compared to GY waters. Moreover, e-ratio values were as high as 9.7 in MA waters, i.e. higher than the e-ratios

6   in most studied oligotrophic regions (Karl et al., 2012; Raimbault and Garcia, 2008), where it rarely exceed 1 %,

7   indicating that production sustained by N_2 fixation is efficiently exported in the WTSP. Diazotrophs were recovered

8   in sediment traps during the cruise (Caffin et al., 2017), but their biomass only accounted for ~5 % (locally 30% at

9   LDA) of the N biomass in the traps, indicating that most of the export was indirect, i.e. after transfer of diazotroph-

10   derived N to the surrounding planktonic communities that were subsequently exported. A δ^{15}N-budget performed

11   during the OUTPACE cruise reveals that N_2 fixation supports exceptionally high (>50 % and locally >80 %) of export

12   production in MA waters (Knapp et al., Submitted). Together these results suggest that N_2 fixation plays a critical role

13   in export in this globally important 'hot spot' of N_2 fixation.

14

15   **5   Conclusions**

16   The magnitude and geographic extent of N_2 fixation control the rate of primary productivity and vertical export of

17   carbon in the oligotrophic ocean, thus accurate estimates of N_2 fixation are of primary importance for oceanographers

18   to constrain and predict the evolution of marine biogeochemical carbon and N cycles. Global N_2 fixation estimates

19   have increased dramatically over the past three decades (Luo et al., 2012). The results of this study show that some

20   poorly explored areas such as the WTSP provide unique conditions for diazotrophs to fix at high rates and may

21   contribute to revise upward the current N_2 fixation estimates for the Pacific Ocean. Further studies would be required

22   along the annual time scale to assess the seasonal variability of N_2 fixation in this region and perform accurate N

23   budgets. Nonetheless, such high N_2 fixation rates question whether or not these high N inputs can balance the N losses

24   in the ETSP. A recent study based on the N* (the excess of N relative to P) at the South Pacific scale (Fumenia et al.,

25   Submitted) reveals a strong positive N* anomaly (indicative of N_2 fixation) in the surface and thermocline waters of

26   the WTSP, which potentially influences the geochemical signature of the thermocline waters further east in the South

27   Pacific through the regional circulation. However, the WTSP is chronically undersampled, and a better description of

28   the mesoscale and general circulation would be necessary to assess how N sources and sinks are coupled at the South

29   Pacific scale.

30

31

32

33

34

35

36

1 **Author contribution**: S.B designed the experiments, S.B. M.C., H.B. and M.B. carried them out at sea. M.C., H.B.,
2 R.A.F., S.H.N. and O.G. analyzed the samples, M.C. and S.B. analyzed the data. S.B. prepared the manuscript with
3 contributions from all co-authors
4
19
20
21
22
23
24
25
26
27
28
29
30
31
32
33
34
35
36
37
38
39

Biogeosciences
Discussions

EGU Open Access

References

Aminot, A., and Kerouel, R.: Dosage automatique des nutriments dans les eaux marines: méthodes en flux continu, in, Quae ed., edited by: Quae, 187 pp, 2007.

Benavides, M., Moisander, P. H., Berthelot, H., Dittmar, T., and Grosso, O.: Mesopelagic N_2 fixation related to organic matter composition in the Solomon and Bismarck Seas (Southwest Pacific), PloS one, 10, doi:10.1371/journal.pone.0143775, 2015.

Benavides, M., and Voss, M.: Five decades of N2 fixation research in the North Atlantic Ocean, Frontiers in Marine Science, 2, 10.3389/fmars.2015.00040, 2015.

Benavides, M., Moisander, P. H., Daley, M. C., Bode, A., and Arístegui, J.: Longitudinal variability of diazotroph abundances in the subtropical North Atlantic Ocean, Journal of Plankton Research, 38, 662-672, 2016.

Benavides, M., Berthelot, H., Duhamel, S., Raimbault, P., and Bonnet, S.: Dissolved organic matter uptake by Trichodesmium in the Southwest Pacific, Scientific Reports, 7, 41315, 10.1038/srep41315 http://www.nature.com/articles/srep41315#supplementary-information, 2017.

Berthelot, H., Bonnet, S., Grosso, O., Cornet, V., and Barani, A.: Transfer of diazotroph-derived nitrogen towards non-diazotrophic planktonic communities: a comparative study between Trichodesmium erythraeum, Crocosphaera watsonii and Cyanothece sp., Biogeosciences, 13, 4005-4021, 10.5194/bg-13-4005-2016, 2016.

Berthelot, H., Benavides, M., Moisander, P. H., Grosso, O., and Bonnet, S.: High nitrogen fixation rates in the particulate and dissolved pools in the Western Tropical Pacific (Solomon and Bismarck Seas), Geophysical Research Letters, 2017.

Blain, S., Bonnet, S., and Guieu, C.: Dissolved iron distribution in the tropical and sub tropical South Eastern Pacific, Biogeosciences, 5, 269–280, 2008.

Bock, N., Van Wambeke, F., Dion, M., and Duhamel, S.: Microbial community structure in the Western Tropical South Pacific, Biogeosciences Discussions, Submitted.

Bonnet, S., Guieu, C., Bruyant, F., Prasil, O., Van Wambeke, F., Raimbault, P., Moutin, T., Grob, C., Gorbunov, M. Y., Zehr, J. P., Masquelier, S. M., Garczarek, L., and Claustre, H.: Nutrient limitation of primary productivity in the Southeast Pacific (BIOSOPE cruise), Biogeosciences, 5, 215-225, 2008.

Bonnet, S., Biegala, I. C., Dutrieux, P., Slemons, L. O., and Capone, D. G.: Nitrogen fixation in the western equatorial Pacific: Rates, diazotrophic cyanobacterial size class distribution, and biogeochemical significance, Global Biogeochemical Cycles, 23, 1-13, doi 10.1029/2008gb003439, 2009.

Bonnet, S., Grosso, O., and Moutin, T.: Planktonic dinitrogen fixation along a longitudinal gradient across the Mediterranean Sea during the stratified period (BOUM cruise), Biogeosciences, 8, 2257-2267, 10.5194/bg-8-2257-2011, 2011.

Bonnet, S., Rodier, M., Turk, K., K., Germineaud, C., Menkes, C., Ganachaud, A., Cravatte, S., Raimbault, P., Campbell, E., Quéroué, F., Sarthou, G., Desnues, A., Maes, C., and Eldin, G.: Contrasted geographical distribution of N2 fixation rates and nifH phylotypes in the Coral and Solomon Seas (South-Western Pacific) during austral winter conditions, Global Biogeochemical Cycles, 29, DOI: 10.1002/2015GB005117, 2015.

Bonnet, S., Berthelot, H., Turk-Kubo, K., Cornet-Barthaux, V., Fawcett, S., Berman-Frank, I., Barani, A., Gregori, G., Dekaezemacker, J., Benavides, M., and Capone, D. G.: Diazotroph derived nitrogen supports diatom growth in the

1 South West Pacific: A quantitative study using nanoSIMS, Limnology and Oceanography, 61, 1549-1562,

2 10.1002/lno.10300, 2016a.

3 Bonnet, S., Berthelot, H., Turk-Kubo, K., Fawcett, S., Rahav, E., L'Helguen, S., and Berman-Frank, I.: Dynamics of

4 N 2 fixation and fate of diazotroph-derived nitrogen in a low-nutrient, low-chlorophyll ecosystem: results from the

5 VAHINE mesocosm experiment (New Caledonia), Biogeosciences, 13, 2653-2673, 2016b.

6 Bonnet, S., Berthelot, H., Turk-Kubo, K., Fawcett, S. E., Rahav, E., L'Helguen, S., and Berman-Frank, I.: Dynamics

7 of N2 fixation and fate of diazotroph-derived nitrogen in a low nutrient low chlorophyll ecosystem: results from the

8 VAHINE mesocosm experiment (New Caledonia)   Biogeosciences, 13, 2653-2673 doi:10.5194/bg-13-2653-2016,

9 2016c.

10 Bonnet, S., Caffin, M., Berthelot, H., and Moutin, T.: Hot spot of N2 fixation in the western tropical South Pacific

11 pleads for a spatial decoupling between N2 fixation and denitrification, Proceedings of the National Academy of

12 Sciences of the United States of America, 114, E2800-E2801, 10.1073/pnas.1619514114, 2017.

13 Böttjer, D., Dore, J. E., Karl, D. M., Letelier, R. M., Mahaffey, C., Wilson, S. T., Zehr, J., and Church, M. J.: Temporal

14 variability of nitrogen fixation and particulate nitrogen export at Station ALOHA, Limnology and Oceanography, 62,

15 200-216, 10.1002/lno.10386, 2017.

16 Boutrif, M., Garel, M., Cottrell, M. T., and Tamburini, C.: Assimilation of marine extracellular polymeric substances

17 by deep-sea prokaryotes in the NW Mediterranean Sea, Environmental microbiology reports, 3, 705-709,

18 10.1111/j.1758-2229.2011.00285.x, 2011.

19 Breitbarth, E., Oschlies, A., and LaRoche, J.: Physiological constraints on the global distribution of *Trichodesmium* -

20 effect of temperature on diazotrophy, Biogeosciences, 4, 53-61, 10.5194/bg-4-53-2007, 2007.

21 Caffin, M., Moutin, T., Foster, R. A., Bouruet-Aubertot, P., Doglioli, A. M., Berthelot, H., Grosso, O., Helias-Nunige,

22 S., Leblond, N., and Gimenez, A.: Nitrogen budgets following a Lagrangian strategy in the Western Tropical South

23 Pacific Ocean: the prominent role of N2 fixation (OUTPACE cruise), Biogeosciences Discussions, in review,

24 https://doi.org/10.5194/bg-2017-468, 2017.

25 Caffin, M., Berthelot, H., Cornet, V., and Bonnet, S.: Transfer of diazotroph-derived nitrogen to phytoplankton and

26 zooplankton in the Western Tropical South Pacific Ocean, Biogeosciences Discussions, Submitted.

27 Carpenter, E. J., Subramaniam, A., and Capone, D. G.: Biomass and primary productivity of the cyanobacterium

28 Trichodesmium spp. in the tropical N Atlantic ocean, deep Sea Research Part I, 51, 173-203, 2004.

29 Dabundo, R., Lehmann, M. F., Treibergs, L., Tobias, C. R., Altabet, M. A., Moisander, A. M., and Granger, J.: The

30 Contamination of Commercial $^{15}N_2$ Gas Stocks with ^{15}N–Labeled Nitrate and Ammonium and Consequences for

31 Nitrogen Fixation Measurements, PloS one, 9, e110335, e110335. doi:10.1371/journal.pone.0110335, 2014.

32 Dekaezemacker, J., and Bonnet, S.: Sensitivity of N_2 fixation to combined nitrogen forms (NO_3^- and NH_4^+) in two

33 strains of the marine diazotroph *Crocosphaera watsonii* (Cyanobacteria), Marine Ecology Progress Series, 438, 33-

34 46, 2011.

35 Dekaezemacker, J., Bonnet, S., Grosso, O., Moutin, T., Bressac, M., and Capone, D. G.: Evidence of active dinitrogen

36 fixation in surface waters of the Eastern Tropical South Pacific during El Nino and La Nina events and evaluation of

37 its potential nutrient controls, Global Biogeochemical Cycles, 27, 1-12, doi:10.1002/gbc.20063, 2013.

1   Deutsch, C., Sarmiento, J. L., Sigman, D. M., Gruber, N., and Dunne, J. P.: Spatial coupling of nitrogen inputs and

2   losses in the ocean, Nature, 445, 163-167, 2007.

3   Dugdale, R. C., and Goering, J. J.: Uptake of New and Regenerated Forms of Nitrogen in Primary Productivity,

4   Limnology and Oceanography, 12, 196-&, DOI 10.4319/lo.1967.12.2.0196, 1967.

5   Dupouy, C., Neveux, J., Subramaniam, A., Mulholland, M. R., Montoya, J. P., Campbell, L., Carpenter, E. J., and

6   Capone, D. G.: Satellite captures Trichodesmium blooms in the southwestern tropical Pacific, EOS, Transactions

7   American Geophysical Union, 81, 13-16, 2000.

8   Dupouy, C., Benielli-Gary, D., Neveux, J., Dandonneau, Y., and Westberry, T. K.: An algorithm for detecting

9   *Trichodesmium* surface blooms in the South Western Tropical Pacific, Biogeosciences, 8, 3631–3647, 2011.

10 Dutheil, C., Aumont, O., Lorrain, A., Gorguès, T., Bonnet, S., Rodier, M., Dupouy, C., Shiozaki, T., and Menkes, C.:

11 Modelling the processes driving Trichodesmium sp. spatial distribution and biogeochemical impact in the tropical

12 Pacific Ocean, Submitted.

13 Eppley, R. W., and Peterson, B. J.: The flux of particulate organic matter to the deep ocean and its relation to planktonic

14 new production, Nature, 282, 677-680, 1979.

15 Falkowski, P. G.: Enzymology of nitrogen assimilation, in: Nitrogen in the marine environment, Elsevier, 839-868,

16 1983.

17 Fernandez, C., Farías, L., and Ulloa, O.: Nitrogen Fixation in Denitrified Marine Waters, PloS one, 6, e20539, 2011.

18 Fernandez, C., González, M. L., Muñoz, C., Molina, V., and Farias, L.: Temporal and spatial variability of biological

19 nitrogen fixation off the upwelling system of central Chile (35–38.5° S), Journal of Geophysical Research: Oceans,

20 120, 3330-3349, 2015.

21 Fitzsimmons, J. N., Boyle, E. A., and Jenkins, W. J.: Distal transport of dissolved hydrothermal iron in the deep South

22 Pacific Ocean, Proceedings of the National Academy of Sciences of the United States of America, 111, 16654-16661,

23 10.1073/pnas.1418778111, 2014.

24 Foster, R. A., Goebel, N. L., and Zehr, J. P.: Isolation of Calothrix rhizosoleniae (cyanobacteria) strain SC01 from

25 Chaetoceros (Bacillariophyta) spp. diatoms of the Subtropical North Pacific Ocean, Journal of Phycology, 45, 1028-

26 1037, 2010.

27 Foster, R. A., Kuypers, M. M. M., Vagner, T., Paerl, R. W., Musat, N., and Zehr, J. P.: Nitrogen fixation and transfer

28 in open ocean diatom-cyanobacterial symbioses, ISME Journal, 5, 1484-1493, 2011.

29 Foster, R. A., Sztejrenszus, S., and Kuypers, M. M. M.: Measuring carbon and N_2 fixation in field populations of

30 colonial and free living cyanobacteria using nanometer scale secondary ion mass spectrometry, Journal of Phycology,

31 49, 502-516, 2013.

32 Fu, F.-X., Yu, E., Garcia, N. S., Gale, J., Luo, Y., Webb, E. A., and Hutchins, D. A.: Differing responses of marine N2

33 fixers to warming and consequences for future diazotroph community structure, Aquatic Microbial Ecology, 72, 33-

34 46, 2014.

35 Fumenia, A., Moutin, T., Bonnet, S., Benavides, M., Petrenko, A., Helias-Nunige, S., and Maes, C.: Nutrient pools

36 and excess nitrogen as a marker of intense dinitrogen fixation in the thermocline water s of the Western Tropical South

37 Pacific Ocean, Submitted.

1   Großkopf, T., Mohr, W., Baustian, T., Schunck, H., Gill, D., Kuypers, M. M. M., Lavik, G., Schmitz, R. A., Wallace,

2   G. W. R., and LaRoche, J.: Doubling of marine dinitrogen-fixation rates based on direct measurements, Nature, 488,

3   361-363, doi:10.1038/nature11338, 2012.

4   Gruber, N.: The marine nitrogen cycle: overview and challenges, Nitrogen in the marine environment, 1-50, 2008.

5   Gruber, N.: Elusive marine nitrogen fixation, Proceedings of the National Academy of Sciences, 113, 4246-4248,

6   2016.

7   Guieu, C., Bonnet, S., Petrenko, A., Menkes, C., Chavaganc, V., Desboeufs, K., and Moutin, T.: Iron from a submarine

8   source impacts the productive layer of the Western Tropical South Pacific Scientific Reports, Under review.

9   Kana, T. M., Darkangelo, C., Hunt, M. D., Oldham, J. B., Bennett, G. E., and Cornwell, J. C.: A membrane inlet mass

10 spectrometer for rapid high precision determination of N_2, O_2, and Ar in environmental water samples, Analytical

11 Chemistry, 66, 4166–4170, 1994.

12 Karl, D. M., Church, M. J., Dore, J. E., Letelier, R., and Mahaffey, C.: Predictable and efficient carbon sequestration

13 in the North Pacific Ocean supported by symbiotic nitrogen fixation, Proceedings of the National Academy of

14 Sciences, 109, 1842–1849, doi: 10.1073/pnas.1120312109, 2012.

15 Klawonn, I., Lavik, G., Böning, P., Marchant, H. K., Dekaezemacker, J., Mohr, W., and Ploug, H.: Simple approach

16 for the preparation of 15− 15N2-enriched water for nitrogen fixation assessments: evaluation, application and

17 recommendations, Frontiers in microbiology, 6, 2015.

18 Knapp, A. N., Dekaezemacker, J., Bonnet, S., Sohm, J. A., and Capone, D. G.: Sensitivity of *Trichodesmium*

19 *erythraeum* and *Crocosphaera watsonii* abundance and N_2 fixation rates to varying NO_3^- and PO_4^{3-} concentrations in

20 batch cultures, Aquatic Microbial Ecology, 66, 223-236, 2012.

21 Knapp, A. N., Casciotti, K. L., Berelson, W. M., Prokopenko, M. G., and Capone, D. G.: Low rates of nitrogen fixation

22 in eastern tropical South Pacific surface waters, Proceedings of the National Academy of Sciences, 113, 4398-4403,

23 2016.

24 Knapp, A. N., McCabe, K., Grosso, O., Leblond, N., Moutin, T., and Bonnet, S.: Distribution and rates of nitrogen

25 fixation in the tropical southwest Pacific Ocean constrained by nitrogen isotope budgets, Submitted.

26 Labatut, M., Lacan, F., Pradoux, C., Chmeleff, J., Radic, A., Murray, J. W., Poitrasson, F., Johansen, A. M., and Thil,

27 F.: Iron sources and dissolved-particulate interactions in the seawater of the Western Equatorial Pacific, iron isotope

28 perspectives, Global Biogeochemical Cycles, doi:10.1002/2014GB004928, 2014.

29 Loescher, C. R., Großkopf, T., Desai, F. D., Gill, D., Schunck, H., Croot, P. L., Schlosser, C., Neulinger, S. C., Pinnow,

30 N., and Lavik, G.: Facets of diazotrophy in the oxygen minimum zone waters off Peru, The ISME journal, 8, 2180-

31 2192, 2014.

32 Luo, Y. W., Doney, S. C., Anderson, L. A., Benavides, M., Bode, A., Bonnet, S., Boström, K. H., Böttjer, D., Capone,

33 D. G., Carpenter, E. J., Chen, Y. L., Church, M. J., Dore, J. E., Falcón, L. I., Fernández, A., Foster, R. A., Furuya, K.,

34 Gómez, F., Gundersen, K., Hynes, A. M., Karl, D. M., Kitajima, S., Langlois, R. J., LaRoche, J., Letelier, R. M.,

35 Maranón, E., McGillicuddy Jr, D. J., Moisander, P. H., Moore, C. M., Mourino-Carballido, B., Mulholland, M. R.,

36 Needoba, J. A., Orcutt, K. M., Poulton, A. J., Raimbault, P., Rees, A. P., Riemann, L., Shiozaki, T., Subramaniam, A.,

37 Tyrrell, T., Turk-Kubo, K. A., Varela, M., Villareal, T. A., Webb, E. A., White, A. E., Wu, J., and Zehr, J. P.: Database

of diazotrophs in global ocean: abundances, biomass and nitrogen fixation rates, Earth System Science Data 5, 47-106, 10.5194/essdd-5-47-2012, 2012.

Martinez-Perez, C., Mohr, W., Loscher, C. R., Dekaezemacker, J., Littmann, S., Yilmaz, P., Lehnen, N., Fuchs, B. M., Lavik, G., Schmitz, R. A., LaRoche, J., and Kuypers, M. M.: The small unicellular diazotrophic symbiont, UCYN-A, is a key player in the marine nitrogen cycle, Nat Microbiol, 1, 16163, 10.1038/nmicrobiol.2016.163, 2016.

Massoth, G., Baker, E., Worthington, T., Lupton, J., de Ronde, C., Arculus, R., Walker, S., Nakamura, K. i., Ishibashi, J. i., and Stoffers, P.: Multiple hydrothermal sources along the south Tonga arc and Valu Fa Ridge, Geochemistry, Geophysics, Geosystems, 8, 2007.

Messer, L. F., Mahaffey, C., M Robinson, C., Jeffries, T. C., Baker, K. G., Bibiloni Isaksson, J., Ostrowski, M., Doblin, M. A., Brown, M. V., and Seymour, J. R.: High levels of heterogeneity in diazotroph diversity and activity within a putative hotspot for marine nitrogen fixation, The ISME journal, 10.1038/ismej.2015.205, 2015.

Messer, L. F., Mahaffey, C., C, M. R., Jeffries, T. C., Baker, K. G., Bibiloni Isaksson, J., Ostrowski, M., Doblin, M. A., Brown, M. V., and Seymour, J. R.: High levels of heterogeneity in diazotroph diversity and activity within a putative hotspot for marine nitrogen fixation, The ISME journal, 10, 1499-1513, 10.1038/ismej.2015.205, 2016.

Mohr, W., Grosskopf, T., Wallace, D. R. W., and LaRoche, J.: Methodological underestimation of oceanic nitrogen fixation rates, PloS one, 9, 1-7, 2010.

Moisander, P. H., Beinart, R. A., Hewson, I., White, A. E., Johnson, K. S., Carlson, C. A., Montoya, J. P., and Zehr, J. P.: Unicellular Cyanobacterial Distributions Broaden the Oceanic N_2 Fixation Domain, Science, 327, 1512-1514, DOI 10.1126/science.1185468, 2010.

Moisander, P. H., Zhang, R. F., Boyle, E. A., Hewson, I., Montoya, J. P., and Zehr, J. P.: Analogous nutrient limitations in unicellular diazotrophs and *Prochlorococcus* in the South Pacific Ocean, ISME Journal, 6, 733-744, DOI 10.1038/ismej.2011.152, 2011.

Monteiro, F. M., Dutkiewicz, S., and Follows, M. J.: Biogeographical controls on the marine nitrogen fixers, Global Biogeochemical Cycles, 25, Artn Gb2003
10.1029/2010gb003902, 2011.

Montoya, J. P., Voss, M., Kahler, P., and Capone, D. G.: A simple, high-precision, high-sensitivity tracer assay for N_2 fixation, Applied and Environmental Microbiology, 62, 986-993, 1996.

Montoya, J. P., Holl, C. M., Zehr, J. P., Hansen, A., Villareal, T. A., and Capone, D. G.: High rates of N_2 fixation by unicellular diazotrophs in the oligotrophic Pacific Ocean, Nature, 430, 1027-1031, DOI 10.1038/nature02824, 2004.

Moore, C. M., Mills, M. M. M., Arrigo, K. R., Berman-Frank, I., Bopp, L., Boyd, P. W., Galbraith, E. D., Geider, R. J., Guieu, C., Jaccard, S. L., Jickells, T. D., La Roche, J., Lenton, T. M., Mahowald, N. M., Maranon, E., Marinov, I., Moore, J. K., Nakatsuka, T., Oschlies, A., Saito, M. A., Thingstad, T. F., Tsuda, A., and Ulloa, O.: Processes and patterns of oceanic nutrient limitation, Nature Geoscience, 6, 701–710, doi:10.1038/ngeo1765, 2013.

Moutin, T., Van Den Broeck, N., Beker, B., Dupouy, C., Rimmelin, P., and LeBouteiller, A.: Phosphate availability controls Trichodesmium spp. biomass in the SW Pacific ocean, Marine Ecology-Progress Series, 297, 15-21, 2005.

Moutin, T., Karl, D. M., Duhamel, S., Rimmelin, P., Raimbault, P., Van Mooy, B. A. S., and Claustre, H.: Phosphate availability and the ultimate control of new nitrogen input by nitrogen fixation in the tropical Pacific Ocean, Biogeosciences, 5, 95-109, 2008.

1   Radic, A., Lacan, F., and Murray, J. W.: Iron isotopes in the seawater of the equatorial Pacific Ocean: New constraints
2   for the oceanic iron cycle, Earth and Planetary Science Letters, 306, 1-10, 2011.

3   Raimbault, P., and Garcia, N.: Evidence for efficient regenerated production and dinitrogen fixation in nitrogen-
4   deficient waters of the South Pacific Ocean: impact on new and export production estimates, Biogeosciences, 5, 323-
5   338, 2008.

6   Raven, J. A.: The iron and molybdenum use efficiencies of plant growth with different energy, carbon and nitrogen
7   source, New Phytologist, 109, 279-287, 1988.

8   Shiozaki, T., Kodama, T., Kitajima, S., Sato, M., and Furuya, K.: Advective transport of diazotrophs and importance
9   of their nitrogen fixation on new and primary production in the western Pacific warm pool, Limnology and
10 Oceanography, 58, 49-60, DOI 10.4319/lo.2013.58.1.0049, 2013.

11 Shiozaki, T., Kodama, T., and Furuya, K.: Large-scale impact of the island mass effect through nitrogen fixation in
12 the western South Pacific Ocean, Geophysical Research Letters, 41, 2907-2913, 2014.

13 Shiozaki, T., Nagata, T., Ijichi, M., and Furuya, K.: Nitrogen fixation and the diazotroph community in the temperate
14 coastal region of the northwestern North Pacific, Biogeosciences, 12, 4751–4764, doi:10.5194/bg-12-4751-2015,
15 2015, 2015.

16 Stenegren, M., Caputo, A., Berg, C., Bonnet, S., and Foster, R. A.: Distribution and drivers of symbiotic and free-
17 living diazotrophic cyanobacteria in the Western Tropical South Pacific, Biosci. Discuss, 1-47, 2017.

18 Tenorio, M., C., D., Rodier, M., and Neveux, J.: Filamentous cyanobacteria and picoplankton in the South Western
19 Tropical Pacific Ocean (Loyalty Channel, Melanesian Archipelago) during an El Nino episode, Aquatic Microbial
20 Ecology, Accepted.

21 Thompson, A. W., Foster, R. A., Krupke, A., Carter, B. J., Musat, N., Vaulot, D., Kuypers, M. M. M., and Zehr, J. P.:
22 Unicellular Cyanobacterium Symbiotic with a Single-Celled Eukaryotic Alga, Science, 337, 1546-1550,
23 10.1126/science.1222700, 2012.

24 Van Wambeke, F., Gimenez, A., Duhamel, S., Dupouy, C., Lefevre, D., Pujo-Pay, M., and Moutin, T.: Dynamics of
25 phytoplankton and heterotrophic bacterioplankton in the western tropical South Pacific ocean along a gradient of
26 diversity and activity of N2-fixing organisms, Biogeosciences Discussions, Submitted.

27 Verity, P. G., Robertson, C. Y., Tronzo, C. R., Andrews, M. G., Nelson, J. R., and Sieracki, M. E.: Relationships
28 between cell volume and the carbon and nitrogen content of marine photosynthetic nanoplankton, Limnology and
29 Oceanography, 37, 1434–1446, doi:10.4319/lo.1992.37.7.1434, 1992, 1992.

30 Weiss, R. F.: The solubility of nitrogen, oxygen and argon in water and seawater, Deep Sea Research, 17, 721-735,
31 1970.

32 Wilson, S. T., Böttjer, D., Church, M. J., and Karl, D. M.: Comparative assessment of nitrogen fixation methodologies
33 conducted in the oligotrophic Noth Pacific Ocean, Applied and Environmental Microbiology, 78, 6516–6523,
34 10.1128/aem.01146-12, 2012.

35
36
37
38

1   **Table 1**. $^{15}N/^{14}N$ ratio of suspended particulate nitrogen (average over the photic layer) across the OUTPACE transect.

2

Station	$^{15}N/^{14}N$ ratio-PN$_{susp}$
#	(‰)
MA waters	
1	2.00
2	0.78
3	0.57
A	-
4	2.71
5	1.57
6	1.91
7	0.5
8	-2.45
9	-2.21
10	-2.7
11	-7.05
12	1.89
B	-2.88
Average MA waters	*-0.41*
GY waters	
C	7.91
14	8.72
15	7.55
Average GY waters	*8.06*

3

4

5

6

7

8

9

10

11

1   **Table 2**. Summary of relationships between N_2 fixation and physical and biogeochemical parameters and among N_2

2   fixation rates and several diazotrophic or non-diazotrophic planktonic groups indicated by Spearman's rank correlation

3   (n=102, α=0.05). The significant correlations ($p<0.05$) are indicated by an asterisk (*).

4

	Variable	Unit	N_2 fixation Spearman's correlation coefficient
Physical and biogeochemical parameters	Pressure	dbar	-0.705*
	Temperature	°C	0.658*
	Salinity	psu	-0.701*
	Oxygen	$\mu mol\ Kg^{-1}$	0,151
	PAR	$\mu mol\ photons\ m^{-2}\ s^{-1}$	0.319*
	NO_3^-	$\mu mol\ L^{-1}$	-0.544*
	NH_4^+	$\mu mol\ L^{-1}$	-0,024
	DIP	$\mu mol\ L^{-1}$	-0.770*
	$Si(OH)_4$	$\mu mol\ L^{-1}$	-0.724*
	DFe	$nmol\ L^{-1}$	0.398*
	DON	$\mu mol\ L^{-1}$	0.517*
	DOP	$\mu mol\ L^{-1}$	0.418*
	DOC	$\mu mol\ L^{-1}$	0.573*
	PON	$\mu mol\ L^{-1}$	0.721*
	POC	$\mu mol\ L^{-1}$	0.723*
	Biogenic silica	$\mu mol\ L^{-1}$	0.274*
	Chl *a*	$\mu g\ L^{-1}$	0.266*
	Primary production	$\mu g\ C\ L^{-1}\ d^{-1}$	0.657*
	Bacterial production	$\mu mol\ C\ L^{-1}\ h^{-1}$	0.692*
	T_{DIP}	days	-0.721*
Planktonic groups	*Trichodesmium* sp.	*nifH* copies L^{-1}	0.729*
	UCYN-A1	*nifH* copies L^{-2}	-0,051
	UCYN-A2	*nifH* copies L^{-3}	-0,147
	UCYN-B	*nifH* copies L^{-4}	0.511*
	het-1	*nifH* copies L^{-5}	0.538*
	het-2	*nifH* copies L^{-6}	0.576*
	het-3	*nifH* copies L^{-7}	0.276*
	Prochlorococcus sp.	cells ml^{-1}	0.697*
	Synechococcus sp.	cells ml^{-1}	0.720*
	Pico-eukaryotes	cells ml^{-1}	-0.450*
	Bacteria	cells ml^{-1}	0.780*
	Protists	cells ml^{-1}	0.680*

5

6

1   **Table 3**. Summary of diazotroph abundances and nanoSIMS analyses at SD2, SD6 and LDB.

Station #	*Trichodesmium* abundance (cells L^{-1})	Contribution to diazotroph community (%)	Atom% ^{15}N (mean ± SD)	N$_2$ fixation rate (fmol cell^{-1} d^{-1})	Contribution to bulk N$_2$ fixation (%)
SD2	1.3×10^5	84.9	0.610 ± 0.269	38.9 ± 8.1	83.8
SD6	3.3×10^5	68.0	0.637 ± 0.355	29.3 ± 5.4	47.1
LDB	1.2×10^5	91.8	0.981 ± 0.466	123.8 ± 24.7	52.9

Station #	*Trichodesmium* abundance (cells L^{-1})	Contribution to diazotroph community (%)	Atom% ^{15}N (mean ± SD)	N$_2$ fixation rate (fmol cell^{-1} d^{-1})	Contribution to bulk N$_2$ fixation (%)
SD2	2.0×10^4	13.2	1.163 ± 0.531	30.0 ± 6.4	10.1
SD6	1.5×10^5	31.7	0.517 ± 0.237	6.1 ± 1.2	6.1
LDB	3.8×10^2	0.3	n.d	n.d	n.d

2

3

4

5

6

7

8

9

10

11

12

13

14

15

16

17

1   **Table 4**. Summary of average *nifH* gene expression data determined by qRT-PCR at selected stations (SD2, SD6,
2   LDB), where the cell-specific N_2 fixation rates were measured.

3

Diazotroph	Station SD2 cDNA *nifH* (gene copies L^{-1})	Station SD6 cDNA *nifH* (gene copies L^{-1})	Station LDB cDNA *nifH* (gene copies L^{-1})
Trichodesmium spp.	1.1×10^5	5.1×10^5	5.78×10^4
UCYN-B	1.9×10^5	1.5×10^5	1.03×10^2
Het-1	6.83×10^2	1.56×10^3	2.04×10^2
Het-2	5.44×10^2	2.14×10^2	bd
UCYN-A1	bd	bd	bd

4

5

6

7

8

9

10

11

12

13

14

15

16

17

18

19

20

21

22

23

24

25

26

27

28

29

30

31

1   **Figure captions**

2

3   **Figure 1.** Upper panel: general situation of the western and central Pacific and associated Seas. Lower panel: Sampling

4   locations superimposed on a composite sea surface Chl *a* concentrations during the OUTPACE cruise (February 19th-

5   April 3rd, quasi-Lagrangian weighted mean Chl *a*). Short- duration (X) and long (+) duration stations are indicated.

6   The satellite data are weighted in time by each pixel's distance from the ship's average daily position for the entire

7   cruise. The white line shows the vessel route (data from the hull-mounted ADCP positioning system). The satellite

8   products are provided by CLS with the support of CNES.

9

10   **Figure 2.** Horizontal and vertical distributions of (a) seawater temperature (°C), (b) fluorescence (μg L^{-1}), (c) NO$_3^-$

11   (μmol L^{-1}), (d) DIP (μmol L^{-1}) and (e) N$_2$ fixation rates (nmol N L^{-1} d^{-1}) across the OUTPACE transect. LD stations

12   are reported as well as the two sub-regions MA: Melanesian archipelago waters, GY: South Pacific Gyre waters. Y

13   axis: pressure (dbar), X axis: longitude, black dots correspond to sampling depths.

14

15   **Figure 3**. (a) ^{15}N/^{14}N ratio of the N$_2$ pool in the incubation bottles incubated either in on-deck incubators (n=54) and

16   in situ (mooring line) (n=44). The dashed line represent the theoretical value (~8.2 atom%) calculated assuming

17   complete isotopic equilibration between the gas bubble and the seawater based on gas constants. (b) Depth profiles of

18   ^{15}N/^{14}N ratio of the N$_2$ pool in the incubation bottles incubated either in on-deck incubators (filled symbols) or on an

19   in situ mooring line (open symbols).

20

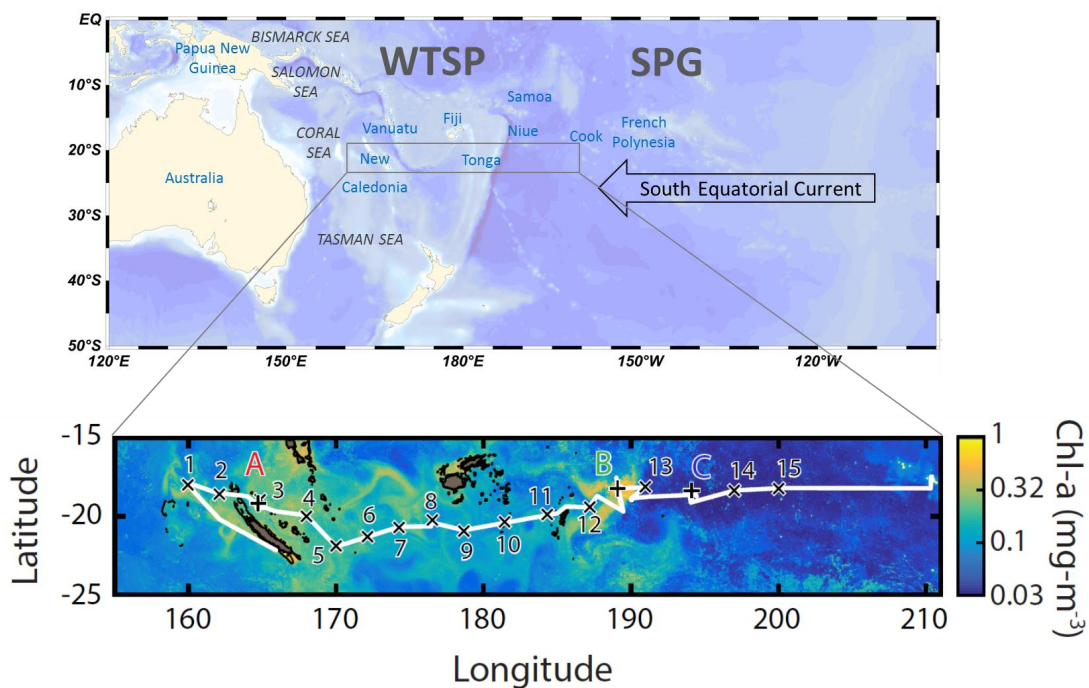21

22

23

24

25

26

27

28
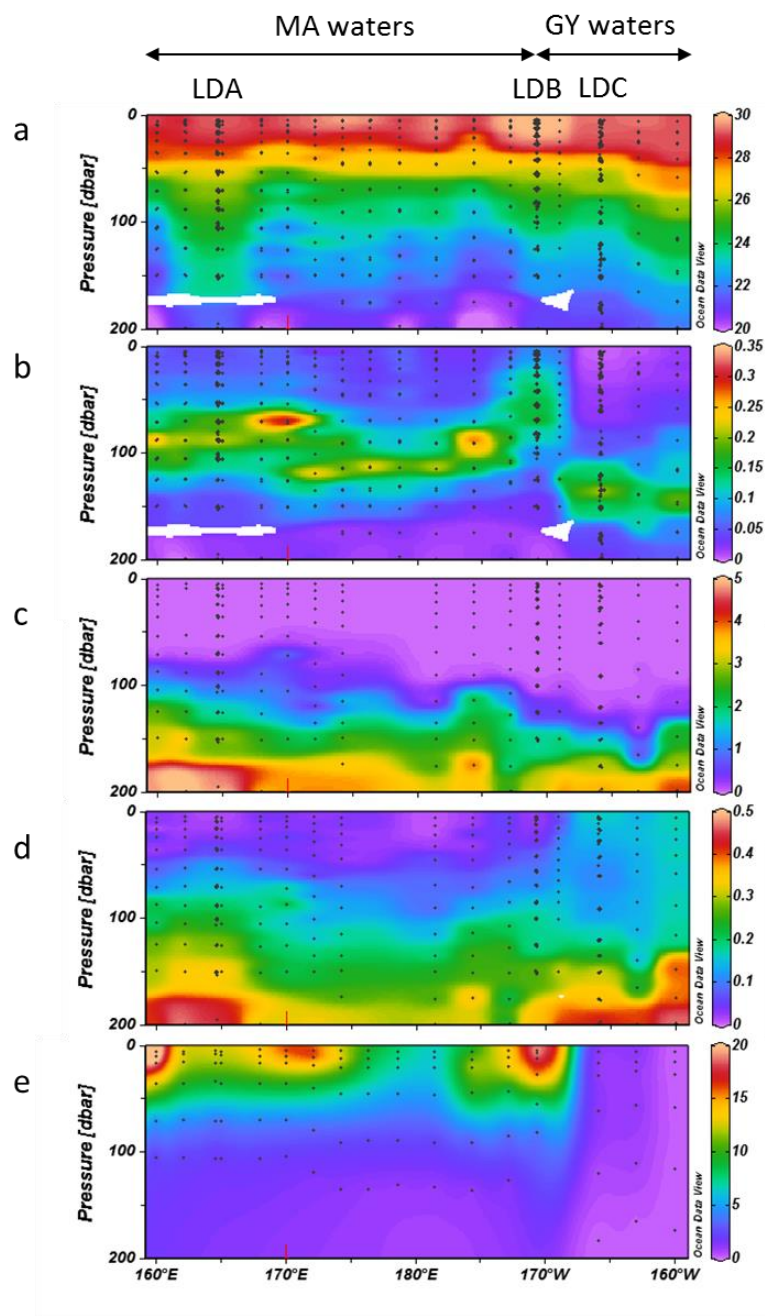
29

30

31

32

33

34

35

36

1

2

3

4

5

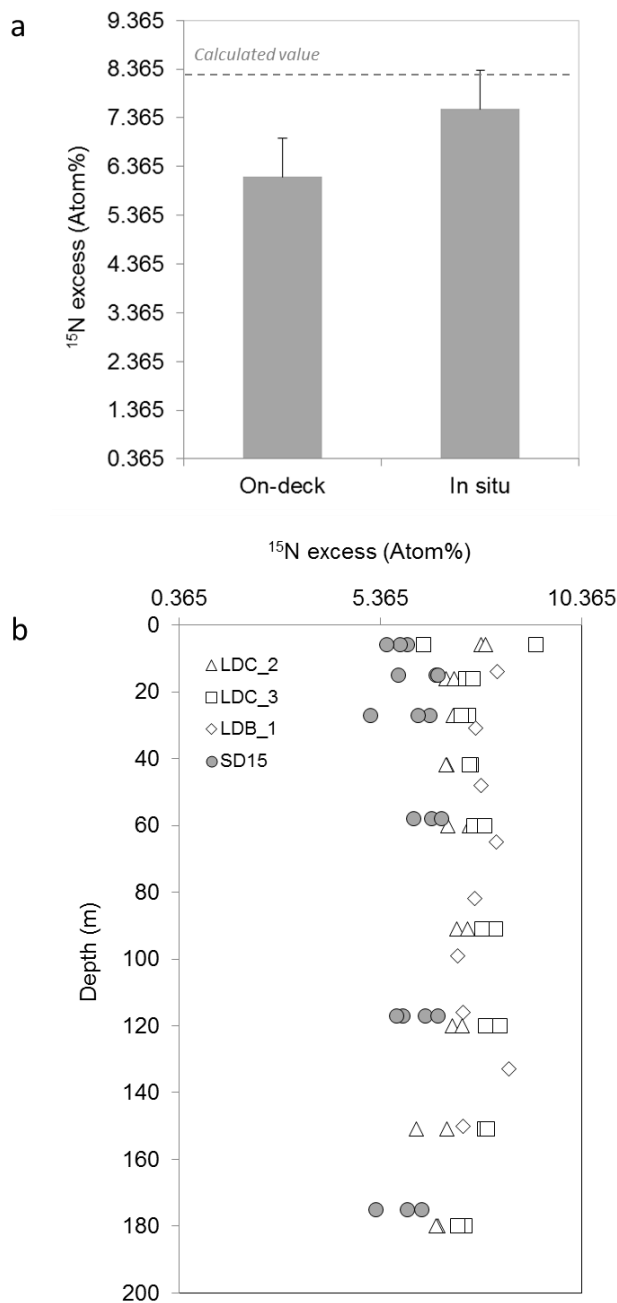6   Figure 1.

7

8

9

1

2

3   Figure 2.

4

Figure 3